Inhibition of Class A and Class C β-Lactamases by Penems: Crystallographic Structures of a Novel 1,4-Thiazepine Intermediate†,‡

Michiyoshi Nukaga,§ Takao Abe,|| Aranapakam M. Venkatesan,⊥ Tarek S. Mansour,⊥ Robert A. Bonomo,@ and James R. Knox*,§

Department of Molecular and Cell Biology, The University of Connecticut, Storrs, Connecticut 06269-3125, Wyeth Lederle Japan, Saitama, Japan, Chemical and Screening Sciences, Wyeth Research, Pearl River, New York 10965, and Research Service, Department of Veterans Affairs Medical Center, Cleveland, Ohio 44106

Received June 9, 2003; Revised Manuscript Received September 11, 2003

ABSTRACT: A new β-lactamase inhibitor, a methylidene penem having a 5,6-dihydro-8*H*-imidazo[2,1-*c*]-[1,4]oxazine heterocyclic substituent at the C6 position with a *Z* configuration, irreversibly inhibits both class A and class C serine β-lactamases with IC_{50} values of 0.4 and 9.0 nM for TEM-1 and SHV-1 (class A), respectively, and 4.8 nM in AmpC (class C) β-lactamases. The compound also inhibits irreversibly the class C extended-spectrum GC1 β-lactamase (IC_{50} = 6.2 nM). High-resolution crystallographic structures of a reaction intermediate of (5*R*)-(6*Z*)-6-(5,6-dihydro-8*H*-imidazo[2,1-*c*][1,4]oxazin-2-ylmethylene)-7-oxo-4-thia-1-azabicyclo[3.2.0]hept-2-ene-3-carboxylic acid **1** with the SHV-1 β-lactamase and with the GC1 β-lactamase have been determined by X-ray diffraction to resolutions of 1.10 and 1.38 Å, respectively. The two complexes were refined to crystallographic *R*-factors (R_{free}) of 0.141 (0.186) and 0.138 (0.202), respectively. Cryoquenching of the reaction of **1** with each β-lactamase crystal produced a common, covalently bound intermediate. After acylation of the serine, a nucleophilic attack by the departing thiolate on the C6′ atom yielded a novel seven-membered 1,4-thiazepine ring having *R* stereochemistry at the new C7 moiety. The orientation of this ring in each complex differs by a 180° rotation about the bond to the acylated serine. The acyl ester bond is stabilized to hydrolysis through resonance stabilization with the dihydrothiazepine ring and by low occupancy or disorder of hydrolytic water molecules. In the class A complex, the buried water molecule on the α-face of the ester bond appears to be loosely bound or absent. In the class C complex, a water molecule on the β-face is disordered and poorly activated for hydrolysis. Here, the acyl intermediate is unable to assist its own hydrolysis, as is thought to occur with many class C substrates.

The bacterial β-lactamase enzymes provide resistance to antibiotics of the β-lactam family (penicillins, cephalosporins, carbapenems, and monobactams) by hydrolyzing the β-lactam bond. The most studied of these enzymes, clinically, biochemically, and structurally, are the serine-reactive β-lactamases in classes A and C (for reviews, see refs *1*−*4*). An approach to combat resistance is to co-administer the enzyme-susceptible β-lactam with a β-lactamase inhibitor. A small number of inhibitors, such as clavulanic acid **2**, sulbactam **3**, and tazobactam **4**, have been heavily employed in the clinic since the mid-1980s (*5*−*7*). However, these compounds display poor inhibition of the class C β-lactamases, and their effectiveness against the class A enzymes has steadily diminished as inhibitor-resistant β-lactamases arise after high inhibitor usage (*8*, *9*).

It is desirable to have a single compound able to inhibit all classes of the serine-reactive β-lactamases. (Inhibition of the zinc-dependent class B enzymes must use a different chemistry.) The development of new serine-directed inhibitors is being advanced by the examination of crystallographic complexes with established or promising inhibitors for β-lactamases of class A (*10*−*14*), class C (*15*−*18*), and, lately, class D (*19*, *20*). Because of their toxicity, instability, or poor transport, however, few of these inhibitors have been introduced into clinical use.

Here, we describe the properties and reaction mechanism of a novel methylidene penem **1** which was found to exhibit significant inhibitory activity against both class A and C serine β-lactamases. To understand the mode of action of this compound and to facilitate refinement of compounds of this type, we have established the high-resolution crystal structures of its reaction intermediate with the SHV-1 and GC1 β-lactamases, which are well-characterized members of the class A and class C families.

MATERIALS AND METHODS

Subcloning and Protein Purification. The SHV-1 β-lactamase gene (bla_{SHV-1}, GenBank entry AF124984) was directionally subcloned into the phagemid vector pBCSK

† This work was supported by a Merit Review Award from the Department of Veterans Affairs to R.A.B. The work was supported in part by Wyeth Research.

‡ Atomic coordinates for the SHV and GC1 complexes have been deposited in the Protein Data Bank at the Research Collaboratory for Structural Bioinformatics at Rutgers University as entries 1ONG and 1ONH.

* To whom correspondence should be addressed. Phone: (860) 486-3133. Fax: (860) 486-4745. E-mail: james.knox@uconn.edu.

§ The University of Connecticut.

|| Wyeth Lederle Japan.

⊥ Wyeth Research.

@ Department of Veterans Affairs Medical Center.

10.1021/bi034986b CCC: $25.00
Published on Web 10/21/2003

Scheme 1: Synthetic Route to **1**

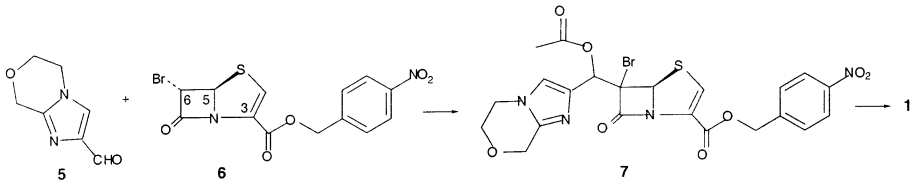

from a clinical strain of *Klebsiella pneumoniae* 15571. *Escherichia coli* DH10B was the host strain used to harvest the SHV-1 enzyme (*21*). The *Enterobacter cloacae* GC1 enzyme was obtained from the GC1 β-lactamase gene on the pCS101 plasmid in *E. coli* AS226-51, as previously described (*22*, *23*).

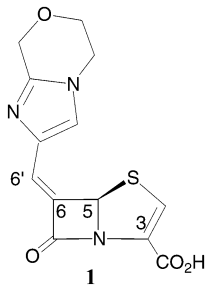

1

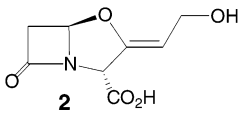

2

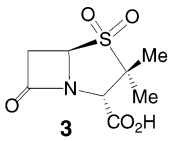

3

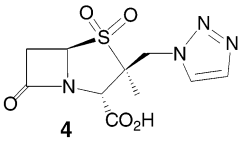

4

*Synthesis and Characterization of (5R)-(6Z)-6-(5,6-Dihydro-8H-imidazo[2,1-c][1,4]oxazin-2-ylmethylene)-7-oxo-4-thia-1-azabicyclo[3.2.0]hept-2-ene-2-carboxylic Acid Sodium Salt **1***. Compound **1** can be synthesized by reacting 5,6-dihydro-8*H*-imidazo[2,1-*c*][1,4]oxazine-2-carboxyaldehyde **5** with 4-nitrobenzyl-(5*R*,6*S*)-6-bromopenem-3-carboxylate **6** under Lewis acid-catalyzed aldol condensation conditions. The methylidene linkage with the *Z* configuration was introduced between the heterocyclic and the penem portions of the molecule by a reductive elimination procedure of aldol intermediate **7**, as shown in Scheme 1 (*24*). Compound **1** was characterized by ^{1}H NMR and mass spectroscopic analysis: ^{1}H NMR (MHz, DMSO-d_6) δ 3.95−4.05 (m, 4H), 4.68−4.78 (q, 2H), 6.32 (s, 1H), 6.50 (s, 1H), 6.95 (s, 1H), 7.54 (s, 1H); M + Na *m*/*z* 328; mp 130 °C.

Crystallization of the Apoenzymes. Ligand-free SHV-1 crystals measuring up to 0.25 mm in all dimensions were grown by the vapor diffusion method. The protein drop [1.5 mg/mL, 0.6 mM Cymal-6[1] detergent (Anatrace, Maume, OH), 15% PEG (M_r = 6000), and 50 mM HEPES buffer (pH 7.0)] was placed over a reservoir solution containing 30% PEG and 100 mM HEPES buffer. The 28.9 kDa SHV-1 enzyme crystallizes in space group $P2_12_12_1$ with one molecule in the asymmetric unit (*21*) and the following cell dimensions: a = 49.6 Å, b = 55.6 Å, and c = 87.0 Å (100 K).

The β-lactamase from *E. cloacae* GC1 was crystallized using the sitting drop vapor diffusion method from a drop (10 mg/mL) containing 10% PEG (M_r = 8000) and 50 mM HEPES (pH 7.0) over a reservoir of 20% PEG in 100 mM HEPES. Streak seeding in a 6 mg/mL protein drop was necessary to produce large crystals. The platelike GC1 crystals are in space group $P2_12_12$ with one molecule of 39.4 kDa in the asymmetric unit (*23*) and the following unit cell parameters: a = 78.0 Å, b = 69.5 Å, and c = 63.1 Å (100 K).

Reaction with Inhibitor. For the SHV-1 enzyme, a pregrown crystal was soaked at room temperature for 3 h in the 30% PEG holding solution (pH 7) containing Cymal-6 and 10 mM **1**, the concentration of which was incrementally increased to minimize cracking. The inhibitor solution was refreshed 15 min before crystal cooling and X-ray data collection. A crystal of the GC1 enzyme was similarly soaked with 2 mM **1** for 70 min.

X-ray Data Collection and Processing. The inhibitor-soaked SHV-1 and GC1 crystals were cryoprotected by the addition of 25% MPD and 25% glycerol, respectively, to each PEG holding solution. Loop-mounted crystals were flash-cooled and kept at 100 K with a nitrogen gas stream (Oxford Cryosystems). One-degree oscillation images were collected on a Q210 CCD detector (Area Detector Systems Corp.) at station A1 of the Cornell High Energy Synchrotron Source (MacCHESS). Only one crystal of each enzyme was used. The high-resolution SHV-1 data were collected before the low-resolution data. The HKL programs (*25*) were used to reduce and scale X-ray intensities (Table 1).

RESULTS

*Properties and Activity of **1***. The purified compound **1**, when incubated with TEM-1 and SHV-1 (class A) or AmpC and GC1 (class C) β-lactamases, effectively inhibited these enzymes with IC_{50} values of 0.4, 9.0, 4.8, and 6.2 nM, respectively. β-Lactamase inhibitory activities (IC_{50} values) were determined spectrophotometrically as described by Bush et al. using nitrocefin (Becton Dickinson, Cockeyville, MD) as the indicator substrate (*26*). Homogeneously purified β-lactamases were prepared from *E. coli* (TEM-1, SHV-1)

[1] Abbreviations: Cymal-6, cyclohexyl (*n*-hexyl)-β-D-maltoside; HEPES, *N*-(2-hydroxyethyl)piperazine-*N*′-(2-ethanesulfonic acid); IC_{50}, concentration of the drug that will result in 50% inhibition of the target enzyme; MIC, concentration of the lowest dilution of the drug in which bacterial growth is absent; MPD, 2-methyl-2,4-pentanediol; PEG, polyethylene glycol; rmsd, root-mean-square deviation.

Table 1: X-ray Data Collection

	SHV-1	GC1
space group	$P2_12_12_1$	$P2_12_12$
cell dimensions (Å)	49.6, 55.2, 85.3	76.3, 68.9, 62.0
temp (K), λ (Å)	100, 0.9349	100, 0.9474
d_{min} (highest-resolution shell) (Å)	1.10 (1.14−1.10)	1.38 (1.43−1.38)
no. of observations	1019910 (30641)	377696 (12765)
no. of unique reflections	87983 (6959)	65047 (5075)
completeness (%)	92.6 (74.2)	97.2 (77.0)
avg $I/\sigma(I)$	14.5 (3.3)	10.5 (2.0)
$R_{sym}(I)$[a]	0.109 (0.374)	0.103 (0.514)

[a] $R_{sym} = \sum|I_{av} - I_i|/\sum I_i$, where I_{av} is the average of all individual observations, I_i.

or *E. cloacae* (AmpC, GC1) and incubated for 5 min with **1**. Enzyme concentrations were as follows: 4.4 nM TEM-1, 26 nM SHV-1, 2.1 nM AmpC, and 5.7 nM GC1. The maximal residual velocity was measured. Compound **1** in combination with piperacillin produced a significant synergistic effect against Gram-positive and Gram-negative isolates, including extended-spectrum β-lactamases and class C-expressing organisms, based on the reduction in MIC values.

Structure Determination and Refinement of the Enzyme Complexes. Initial rigid-body refinement was accomplished with CNS (*27*) beginning with the unliganded SHV-1 (PDB entry 1SHV) and GC1 (PDB entry 1GCE) molecules. A simulated annealing protocol with 2 Å data and cross validation using R_{free} (*28*) were then used in the refinements. XtalView (*29*) was employed for structure and map displays and for manual manipulation of the structures. At this stage, *R*-factors were ca. 35% for the unhydrated SHV-1 and GC1 apoprotein models.

As the protein model was being optimized and hydrated, a large serine-bound ring structure became clear in the difference density of both complexes. Early chemical work with related penems (*30*, *31*) suggested that a seven-member ring compound **13** can be formed by nucleophilic attack of a thiolate leaving group on C6′ (Scheme 2). Intermediate **13** was therefore added to the model of each complex. Because the ring has three tautomeric forms, only weak refinement restraints were applied to the geometry of the ring.

The final stages of the refinement (Tables 2 and 3) were performed with SHELX (*32*) using all $F > 0\sigma(F)$ data and in steps to the highest resolution. Near 1.4 Å resolution, the introduction of anisotropic *B*-factors in both models produced a 1−3% drop in the R_{free} values. Riding hydrogen atoms were later added in calculated positions. In the higher-resolution SHV-1 complex, it was possible to model minor chemical changes resulting from radiation damage (*33*−*35*), viz., partial rupture of the Cys77−Cys123 disulfide bond (ca. 30%), and 20−40% decarboxylation of eight acidic side chains. Similar changes were observed in the extended-spectrum SHV-2 enzyme at ultrahigh (0.9 Å) resolution (*36*).

Ramachandran analysis of the SHV-1 and GC1 protein models showed 92.2 and 92.1% of the residues, respectively, fall in the most favored regions, with none in disallowed regions. For the GC1 enzyme, two main chain pathways were modeled for part of the Ω loop from Leu219 to Gly225. Each path was refined with an occupancy of 0.5. Residues Gly217 and Met218 in the apo-like path were not clear in the map and were omitted. The mixed α,β tertiary structure of each β-lactamase molecule is pictured in Figure 1. The electron density of reaction intermediate **13** in each enzyme is shown in Figure 2. Of the three possible tautomeric forms of the thiazepine ring, **13c** is estimated to be a minor form because very little nonplanarity is seen at C6. The absolute configuration at C7 (initially C6′) is *R*.

Comparison with Apoenzyme Structures. An overlay of the SHV-1 complex with the crystal structure of the unliganded enzyme (1SHV) shows that the side chain of Tyr105 now exhibits two conformations, one apo-like and the other rotated 20° about the $C_\alpha-C_\beta$ axis to bring its ring over the C7 heterocyclic ring of the inhibitor. Glu166 and

Scheme 2: Proposed Reaction of Penem **1** with the Catalytic Serine of Class A and Class C β-Lactamases[a]

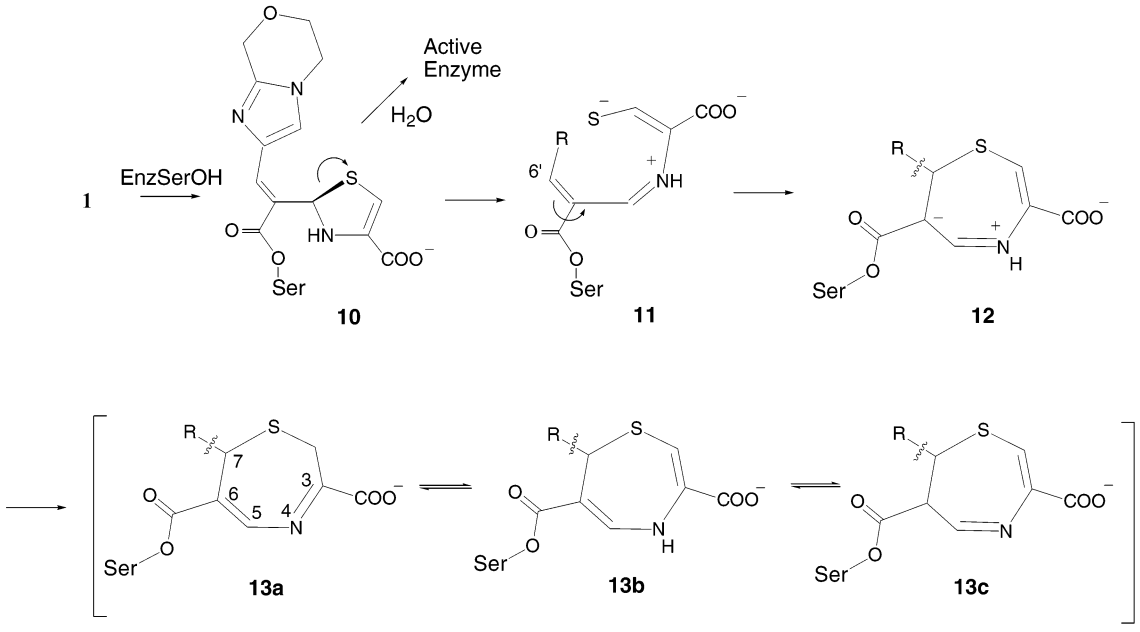

[a] Only one of several thiolate conformations is drawn for intermediate **11**. Species **13** is observed in crystal structures of both enzymes.

Table 2: Structure Solution and Refinement Process for the SHV-1 and GC1 Complexes

refinement step	*d* range (Å)	R/R_{free} (%)	no. of data/ no. of parameters	no. residues with two conformations	no. of waters
		SHV-1 Complex			
rigid body refinement with apo structure	50−2.0	36/37		0	0
begin simulated annealing	50−1.9	23.2/27.2		0	0
increase resolution; add inhibitor and water finish CNS refinement	50−1.2	20.7/23.1		1	159
begin SHELX CGLS refinement	30−1.2	21.1/24.2	69105/8852	1	159
finish isotropic refinement	20−1.07	20.3/23.6	87728/9132	4	210
add anisotropic *B*-factors	20−1.07	16.2/20.1	87728/20522	4	210
add hydrogen atoms and more waters	20−1.10	14.2/18.6	84882/22564	26	296
add waters and conformers	20−1.10	14.1/18.6	84882/22746	29	310
finish SHELX using R_{free}					
add data excluded for R_{free} calculation	20−1.10	14.1	88320/22711	29	301
		GC1 Complex			
rigid body refinement with apo structure	50−2.0	34.5/33.8		0	0
begin simulated annealing	50−1.9	25.8/28.4		0	0
increase resolution; add inhibitor and water finish CNS refinement	50−1.35	19.9/22.3		10 + Ω loop (7)	327
begin SHELX CGLS refinement	20−1.38	19.5/23.2	63533/13011	16 + Ω loop (7)	327
finish isotropic refinement		18.9/22.8	63533/13239		381
add anisotropic *B*-factors	20−1.38	15.4/21.7	63533/29762	16 + Ω loop (7)	381
add hydrogen atoms and more waters	20−1.38	13.9/20.4	63533/30190	19 + Ω loop (7)	424
additional waters and conformers	20−1.38	13.5/20.2	63533/30529	21 + Ω loop (7)	443
finish SHELX using R_{free}					
add data excluded for R_{free} calculation	20−1.38	13.8	65596/30398	21 + Ω loop (7)	428

Table 3: Results from SHELX Refinements

	SHV-1	GC1
resolution range (Å)	20−1.10	20−1.38
no. of reflections used [$F > 0\sigma(F)$]	88320	65596
R-factor (%)[a]	14.1	13.8
R_{free}	18.6	20.2
residues in Ramachandran zones (%)		
favored	92.2	92.1
allowed	7.8	7.9
disallowed	0	0
rms deviations from ideality		
bond lengths (Å)	0.014	0.010
bond angles (Å)	0.032	0.028
planarity (Å^3)	0.081	0.060
mean *B*-factors (Å^2)		
protein	15.3	16.5
intermediate **13** (occupancy)	36.1 (0.63)	17.8 (0.77)
water molecules (no.)	32.6 (301)	35.7 (428)
all atoms (no.)	17.5 (2518)	18.6 (3375)

[a] All data were used to calculate final *R*, including the R_{free} set.

its hydrogen-bonded water molecule W501 are closer (2.3−2.4 Å) than in the apoenzyme, with the water density unresolved from the carboxylate density. This important hydrolytic water molecule is likely to be disordered in the complex, and it refined to an occupancy of only 0.5.

The overlay of the GC1 complex with the apo structure (1GCE) shows that one of the two pathways of the Ω loop follows the apo path, while the second pathway has somewhat better density and follows the path seen in another GC1 complex with a cephem inhibitor (*18*). The Tyr224 in this loop is the side chain most likely to contact the inhibitor during the acylation reaction (Scheme 2), and it is found to be displaced ~6 Å relative to its apo position. Presumably, a composite of inhibited and uninhibited enzyme molecules exists in the crystal lattice. Accordingly, the occupancy of the inhibitor intermediate **13** is less than full (0.77).

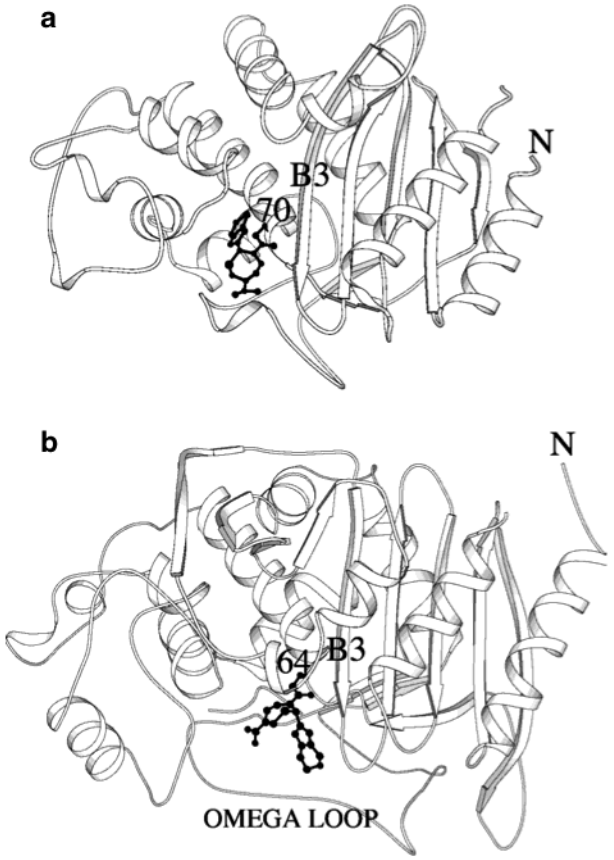

FIGURE 1: Tertiary structure of the complexes with (a) the class A SHV-1 β-lactamase and (b) the class C GC1 β-lactamase. Part of a second pathway is shown for the Ω loop in the GC1 enzyme. In each complex, intermediate **13** is covalently bound in the active site to the reactive serine. Drawn with MOLSCRIPT (*52*).

DISCUSSION

Design Rationale for the Penem Inhibitor. Previous studies involving a series of 6-heterocyclylmethylenepenems identi-

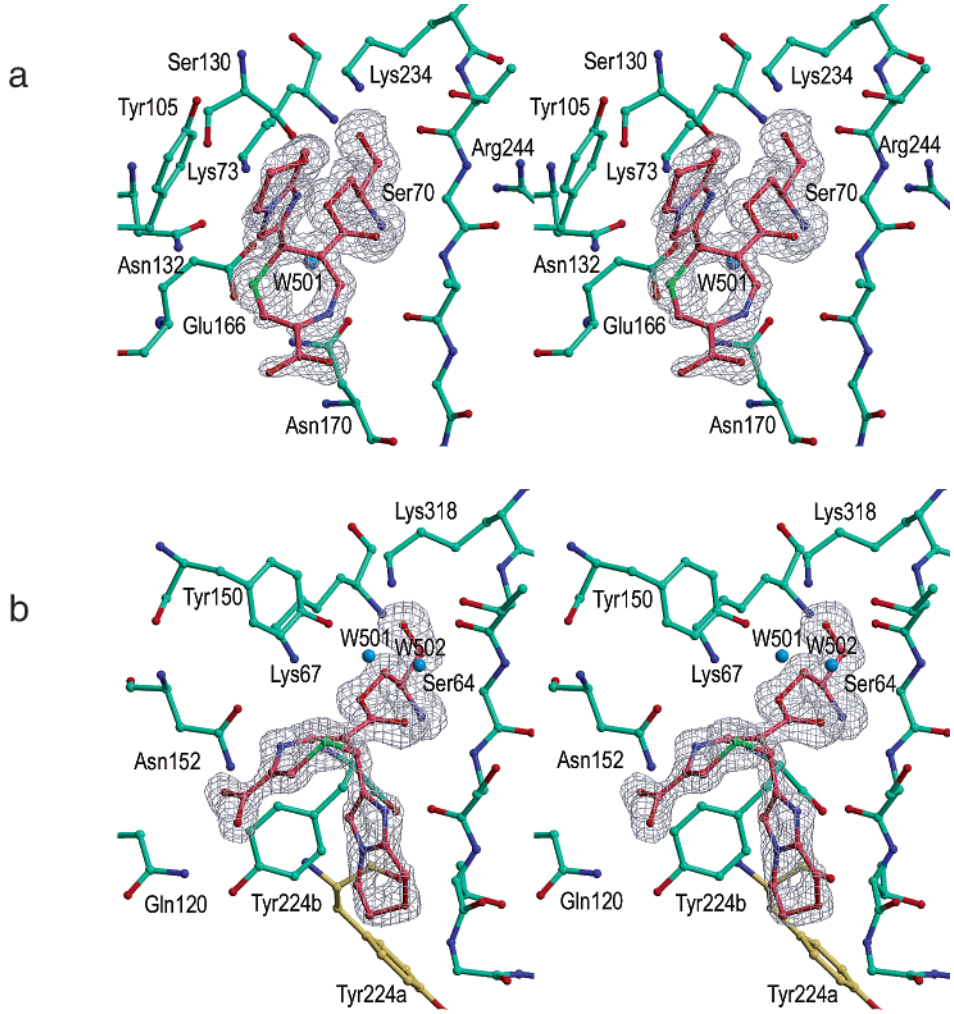

FIGURE 2: Stereoview of the $F_o - F_c$ electron density of intermediate **13** covalently bonded to the reactive serine in (a) the SHV-1 β-lactamase at a contour level of 2.5σ and (b) the GC1 β-lactamase at a contour level of 5.0σ. Two positions of Tyr224 result from two pathways of the Ω loop. The position of Tyr224b is near its position in the apoenzyme. This view angle is similar to that in Figure 1. The figure was made with XtalView (*29*) and Raster3D (*53*).

fied (5*R*)-(2)-6-(1-methyl-1,2,3-triazol-4-ylmethylene)penem-3-carboxylic acid (**8**, BRL-42715) as a potent broad-spectrum β-lactamase inhibitor with a good synergistic effect against a broad range of β-lactamase-producing bacteria (*37*). Extensive structure−activity relationships of the five-membered heterocycles revealed that a high level of β-lactamase inhibitory activity was obtained with several heterocycles (*38*, *39*). We reasoned that bicyclic heterocycles containing a saturated terminal ring in the 6-methylidene substituent and having the *Z* configuration can further enhance binding with TEM-1 (class A) and AmpC (class C) enzymes at the Glu104 and Tyr105 or Gln120 and Tyr221 residues, respectively, assuming acylation at the catalytic serine of each enzyme. SYN-1012 (**9**), a potent broad-spectrum β-lactamase inhibitor which has the same penem and methyl triazolyl substitution at the C6 position as **8** but differs with the latter by having an extended two-carbon linker, demonstrates broad spectrum activity and good synergy with many antibiotics (*40*).

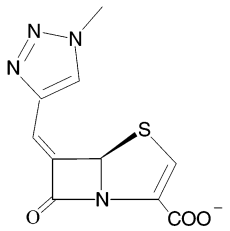

8

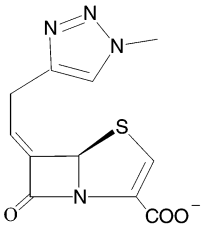

9

Inhibition Pathway. A mechanism for the conversion of penem **1** to the enzyme-bound form observed here is given in Scheme 2. Initial acylation of the reactive serine (Ser70 or Ser64) of the class A or class C β-lactamase produces species **10**, which is thought to hydrolyze rapidly and is therefore short-lived (*31*, *41*). Following the acylation event, rotation about the C5−C6 bond must occur to orient the incipient thiolate for the proper attack at the C6−C6′ double bond (*31*). Ring opening of **10** produces a reactive thiolate species **11** (*30*). Of the several conformations possible in the thiolate, a conformer with *EZZ* double bond configurations is more likely to undergo a 7-*endo-trig* cyclization,

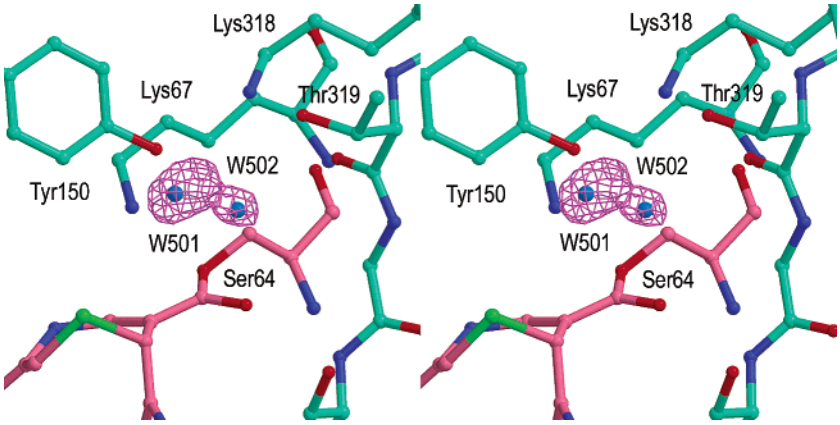

FIGURE 3: Stereoview of the $F_o - F_c$ electron density above the acyl−serine bond of the class C GC1 complex. The contour level is 5σ. Modeled water molecules W501 and W502, each at half-occupancy, are shown.

instead of a 6-*exo-trig* process, to produce thiazepine ring **12**. Attack at the C6−C6′ double bond from either side to produce a dihydrothiazepine is influenced by constraints within the enzyme binding site which affect the chirality outcome at C7 (initially C6′). Dihydrothiazepine **12** has its negative charge stabilized by the acylated carboxylate and the azaallylic moiety. This intermediate is the ion pair of tautomeric 2,7-dihydro-, 4,7-dihydro-, and 6,7-dihydro-1,4-thiazepines **13a**−**13c**, respectively. Because there is little nonplanarity in the electron density map at C6, we estimate the contribution of tautomer **13c** is minor.

Chemical Structure of the Bound Intermediate. Dihydrothiazepine species **13** has been trapped by cryocrystallography in both β-lactamases, and there is no evidence of linear species **11**. It is conceivable that **11** could be present as a minor component in our crystallographic complex, but prior modeling and thiol titration in the solution reaction of the related penem **8** indicated that the linear species is not stabilized in class A and class C binding sites (*31*). The C3 and C6 atoms have sp^2 planarity, and the stereogenic C7 atom has the *R* configuration. There is no evidence in the electron density maps that more than 10−15% of the *S* stereoisomer of **13** was formed by the attack of the thiolate on the opposite face of the double bond in species **11**. This indicates that early steps of the inhibition reaction follow the same conformational pathway in each type of β-lactamase and utilize similar transition states.

Orientation of the Intermediate in the Binding Site. The β-lactam binding sites in the class A and class C β-lactamases have many structural features and conserved residues in common (*42*, *43*), as seen in Figure 2. Here, as in other, but not all (*13*), serine-bound complexes, the β-lactamyl carbonyl group is bound in the oxyanion hole formed by amide groups of the reactive serine and β-strand B3. The dihydrothiazepine rings in the two complexes are generally in the same position, but they differ by a 180° rotation about the connecting bond to the serine ester. In the class A enzyme, the ring lies above the polar side chain of Asn170, and the heterocyclic substituent at C7 lies near the aromatic ring of Tyr105. In the class C binding site, the thiazepine ring is near hydropbobic side chains (Leu119 and Leu296), but the heterocyclic group is directed down along the B3 β-strand. This rotameric preference may be driven by the relative openness of the class C binding site at the bottom of β-strand B3. Rotation of the heterocyclic substituent about the C7−C6 bond differs somewhat from one enzyme to the other. The N atom of the imidazole ring hydrogen bonds to a water molecule in the class C binding site, but in the class A site, the N atom is positioned over the carbon atom of the ester carbonyl group.

In both complexes, we find that the C3 carboxylic acid group of the ring is generally directed outward and has few interactions with the enzyme, especially in the class A structure where the carboxylate group is somewhat disordered and probably solvated. In the class C complex, however, the carboxylate group is well-ordered with a hydrogen bond to the side chain of Gln120 and to a water molecule. In the class A β-lactamase, the N4 atom in the thiazepine ring has very weak interactions (3.3−3.5 Å) with a water molecule and with the main chain carbonyl oxygen atom of residue 237 on β-strand B3. The N4 atom of the class C intermediate points instead to the amine of the Asn152 side chain (3.5 Å).

Our crystallographic results with **1** can be compared with the results of earlier chemical and modeling studies of the reaction of the related penem inhibitor **8** with both class A and class C β-lactamases (*30*, *31*, *41*). The studies correctly predicted the ring expansion rearrangement resulting in the formation of the 1,4-thiazepine ring observed here in both crystal complexes. One study (*31*) went further to use energy minimization to dock a model of **11** and **13** in the binding sites of the class A TEM-1 and class C P99 β-lactamases, both enzymes essentially equivalent to the β-lactamases used here. The docking indicated that only the *S* stereochemistry could be accommodated at C7 in **13**, and it predicted interactions between the ring's C3 carboxylic acid group and the guanidinium group of Arg244 and the hydroxyl group of Ser235 (in class A) or with Asn349 and Thr319 in the class C enzyme. None of the predicted interactions (*31*) is seen in our crystal structures because of the *R* configuration at C7, and because the actual orientation of the thiazepine ring causes the C3 carboxylic acid to be more exposed to solvent.

Stability of the Intermediate. Each class of β-lactamase is generally believed to use a different mechanism for the hydrolysis of the acyl−serine bond (*2*). In class A enzymes, a buried crystallographic water molecule is activated by Glu166 for attack on the α-face of the acyl intermediate. In class C enzymes, the water attacks from the more external β-face and is activated either by the phenoxide of Tyr150 (*15*, *44*) or by substrate assistance via the C3 carboxylic acid group, and with N4 acting as the general base (*45*−*47*). It is

notable that in both complexes described here the inhibitor does not provide steric hindrance to its own hydrolysis, as seen in some other stable acyl complexes. For example, in a class A complex with cefoxitin, the buried hydrolytic water molecule is displaced by the 7β-carbonyl group of the acyl intermediate (*48*), and in a complex with a 6α-substituted penicillanate, the water molecule, though present, is blocked by the 6α substituent of the intermediate (*49*). In some class C complexes, the inhibiting intermediate is found to block the approach of a water molecule to the β-face of the ester bond (*16*, *18*).

We find that in the class A SHV-1 complex no part of intermediate **13** lies near the water position on the α-face of the ester bond, so the disordered, or low-occupancy, hydrolytic water molecule might somehow have been disrupted during the acylation or rearrangement steps of the inhibition reaction (Scheme 2). In the class C complex, the hydrolysis geometry is also defective. The intermediate itself does not obstruct the approach of water to the β-face of the bond, but a single, well-defined water is not seen. Bimodal electron density 3.2 Å from the ester bond was modeled as two half-occupancy water molecules (W501 and W502) only 2 Å apart (Figure 3). W501 forms a bridge to the hydroxyl group of Tyr150 at 3 Å, but at a 90° angle, and is poorly positioned for activation by Tyr150.

Another stabilizing mechanism is observed in some acyl complexes of both classes, whereby the carbonyl oxygen atom of the ester is unable to bind in the oxyanion hole (*13*, *50*, *51*), as required for the tetrahedral transition state in deacylation. This is not the situation here, for we find oxyanion hole binding in both complexes.

For each thiazepine complex, therefore, we conclude that the stability of the serine ester bond to hydrolysis is due to the low occupancy or disorder of the hydrolytic water molecule and, in part, to the conjugation of the ester with the dihydrothiazepine ring system. Further, for the class C complex, the orientation of the dihydrothiazepine ring does not permit its C3 carboxylic acid group and N4 atom to aid the enzyme's Tyr150 in activating the hydrolytic water molecule, providing support for the hypothesis of substrate-assisted deacylation in the class C β-lactamases (*45*−*47*).

ACKNOWLEDGMENT

Preliminary X-ray diffraction data were collected at the Institute of Materials Science of The University of Connecticut. High-resolution data were obtained at the Cornell High Energy Synchrotron Source (CHESS), which is supported by the NSF through Grant DMR-9311772, using the Macromolecular Diffraction facility (MacCHESS), which is supported by NIH Grant RR-01646.

REFERENCES

1. Micetich, R. G., Salama, S. M., Maiti, S. N., Reddy, A. V. N., and Singh, R. (2002) *Curr. Med. Chem.: Anti-Infect. Agents 1*, 193−213.
2. Frere, J.-M. (1995) *Mol. Microbiol. 16*, 385−395.
3. Bush, K., and Mobashery, S. (1998) in *Resolving the Antibiotic Paradox* (Rosen, B., and Mobashery, S., Eds.) pp 71−98, Kluwer Academic/Plenum Publishers, New York.
4. Pratt, R. F. (2002) *J. Chem. Soc., Perkin Trans. 2*, 851−861.
5. Page, M. I., and Laws, A. P. (1998) *Chem. Commun.*, 1609−1617.
6. Page, M. G. P. (2000) *Drug Resist. Updates 3*, 109−125.
7. Sandanayaka, V. P., and Prashad, A. S. (2002) *Curr. Med. Chem. 9*, 1145−1165.
8. Yang, Y., Rasmussen, B. A., and Shlaes, D. M. (1999) *Pharmacol. Ther. 83*, 141−151.
9. Matagne, A., Dubus, A., Galleni, M., and Frere, J.-M. (1999) *Nat. Prod. Rep. 16*, 1−19.
10. Chen, C. C. H., and Herzberg, O. (1992) *J. Mol. Biol. 224*, 1103−1113.
11. Maveyraud, L., Massova, I., Birck, C., Miyashita, K., Samama, J.-P., and Mobashery, S. (1996) *J. Am. Chem. Soc. 118*, 7435−7440.
12. Strynadka, N. C. J., Martin, R., Jensen, S. E., Gold, M., and Jones, J. B. (1996) *Nat. Struct. Biol. 3*, 688−695.
13. Maveyraud, L., Mourey, L., Kotra, L. P., Pedelacq, J.-D., Guillet, V., Mobashery, S., and Samama, J.-P. (1998) *J. Am. Chem. Soc. 120*, 9748−9752.
14. Kuzin, A. P., Nukaga, M., Nukaga, Y., Hujer, A. M., Bonomo, R. A., and Knox, J. R. (2001) *Biochemistry 40*, 1861−1866.
15. Oefner, C., D'Arcy, A., Daly, J. J., Gubernator, K., Charnas, R. L., Heinze, I., Hubschwerfen, C., and Winkler, F. K. (1990) *Nature 343*, 284−288.
16. Heinze-Krauss, I., Angehrn, P., Charnas, R. L., Gubernator, K., Gutknecht, E. M., Hubschwerlen, C., Kania, M., Oefner, C., Page, M. G. P., Sogabe, S., Specklin, J.-L., and Winkler, F. K. (1998) *J. Med. Chem. 41*, 3961−3971.
17. Powers, R. A., Blazquez, J., Weston, G. S., Morosini, M.-I., Baquero, F., and Shoichet, B. K. (1999) *Protein Sci. 8*, 2330−2337.
18. Crichlow, G. V., Nukaga, M., Doppalapudi, V. R., Buynak, J. D., and Knox, J. R. (2001) *Biochemistry 40*, 6233−6239.
19. Pernot, L., Frenois, F., Rybkine, T., L'Hermite, G., Petrella, S., Delettre, J., Jarlier, V., Gollatz, E., and Sougakoff, W. (2001) *J. Mol. Biol. 310*, 859−874.
20. Maveyraud, L., Golemi-Kotra, D., Ishiwata, A., Meroueh, O., Mobashery, S., and Samama, J.-P. (2002) *J. Am. Chem. Soc. 124*, 2461−2465.
21. Kuzin, A. P., Nukaga, M., Nukaga, Y., Hujer, A. M., Bonomo, R. A., and Knox, J. R. (1999) *Biochemistry 38*, 5720−5727.
22. Nukaga, M., KiKuo, T., Yamaguchi, H., and Sawai, T. (1994) *Antimicrob. Agents Chemother. 38*, 1374−1377.
23. Crichlow, G. V., Kuzin, A. P., Nukaga, M., Sawai, T., and Knox, J. R. (1999) *Biochemistry 38*, 10256−10261.
24. Abe, T., Ushirogochi, H., Yamamura, I., Kumagai, T., Mansour, T. S., Venkatesan, A. M., Agarwal, A., Petersen, P. J., Weiss, W. J., Lenoy, E., Yang, Y., and Shlaes, D. (2003) 43rd Annual ICAAC Meeting on Infectious Diseases, Chicago, IL.
25. Otwinowski, Z., and Minor, W. (1997) *Methods Enzymol. 276*, 307−326.
26. Bush, K., Macalintal, C., Rasmussen, B. A., Lee, V. J., and Yang, Y. (1993) *Antimicrob. Agents Chemother. 37*, 851−858.
27. Brunger, A. T., Adams, P. D., Clove, G. M., Delano, W. L., Gros, P., Grosse-Kunstleve, R. W., Jiang, J.-S., Kuszewski, J., Nilges, M., Pannu, N. S., Read, R. J., Rice, L. M., Simonson, T., and Warren, G. L. (1998) *Acta Crystallogr. D54*, 905−921.
28. Brunger, A. T. (1992) *Nature 355*, 472−475.
29. McRee, D. E. (1999) *J. Struct. Biol. 125*, 156−165.
30. Broom, N. J. P., Farmer, T. H., Osborne, N. F., and Tyler, J. W. (1992) *J. Chem. Soc., Chem. Commun.*, 1663−1664.
31. Bulychev, A., Massova, I., Lerner, S. A., and Mobashery, S. (1995) *J. Am. Chem. Soc. 117*, 4797−4801.
32. Sheldrick, G. M., and Schneider, T. R. (1997) *Methods Enzymol. 277*, 319−343.
33. Ravelli, R. B. G., and McSweeney, S. M. (2000) *Structure 8*, 315−328.
34. Leiros, H. S., McSweeney, S. M., and Smalas, A. O. (2001) *Acta Crystallogr. D57*, 488−497.
35. O'Neill, P., Stevens, D. L., and Garman, E. F. (2002) *J. Synchrotron Radiat. 9*, 329−332.
36. Nukaga, M., Mayama, K., Hujer, A. M., Bonomo, R. A., and Knox, J. R. (2003) *J. Mol. Biol. 328*, 289−301.
37. Osbourne, N. F., Atkins, R. J., Broom, N. J. P., Coulton, S., Harbridge, J. B., Harris, M. A., Stirling-Francois, I., and Walker, G. (1994) *J. Chem. Soc., Perkin Trans. 1*, 179−188.
38. Bennett, I., Brooks, G., Broom, N. J. P., Calvert, S., Colemen, K., and Francois, I. (1991) *J. Antibiot. 44*, 969−978.
39. Bennett, I., Broom, N. J. P., Bruton, G., Calvert, S., Clarke, B. P., Colemen, K., Edmondson, R., Edwards, P., Jones, D., Osborne, N. F., and Walker, G. (1991) *J. Antibiot. 44*, 331−343.
40. Phillips, O. A., Czajkowski, D. P., Spevak, P., Singh, M. P., Hanehara-Kunugita, C., Hyodo, A., Micetich, R. G., and Maiti, S. N. (1997) *J. Antibiot. 50*, 350−356.

41. Matagne, A., Ledent, P., Monnaie, D., Felici, A., Jamin, M., Raquet, X., Galleni, M., Klein, D., Francois, I., and Frere, J.-M. (1995) *Antimicrob. Agents Chemother. 39*, 227−231.
42. Lobkovsky, E., Moews, P. C., Liu, H., Zhao, H., Frere, J.-M., and Knox, J. R. (1993) *Proc. Natl. Acad. Sci. U.S.A. 90*, 11257−11261.
43. Knox, J. R., Moews, P. C., and Frere, J.-M. (1996) *Chem. Biol. 3*, 937−947.
44. Lobkovsky, E., Billings, E. M., Moews, P. C., Rahil, J., Pratt, R. F., and Knox, J. R. (1994) *Biochemistry 33*, 6762−6772.
45. Ishiguro, M., and Imajo, S. (1996) *J. Med. Chem. 39*, 2207−2218.
46. Bulychev, A., Massova, I., Miyashita, K., and Mobashery, S. (1997) *J. Am. Chem. Soc. 119*, 7619−7625.
47. Patera, A., Blaszczak, L. C., and Shoichet, B. K. (2000) *J. Am. Chem. Soc. 122*, 10504−10512.
48. Fonze, E., Vanhove, M., Dive, G., Sauvage, E., Frere, J.-M., and Charlier, P. (2002) *Biochemistry 41*, 1877−1885.
49. Mourey, L., Miyashita, K., Swaren, P., Bulychev, A., Samama, J.-P., and Mobashery, S. (1998) *J. Am. Chem. Soc. 120*, 9382−9383.
50. Swaren, P., Massova, I., Bellettini, J. R., Bulychev, A., Maveyraud, L., Kotra, L. P., Miller, M. J., Mobashery, S., and Samama, J.-P. (1999) *J. Am. Chem. Soc. 121*, 5353−5359.
51. Beadle, B. M., and Shoichet, B. K. (2002) *Antimicrob. Agents Chemother. 46*, 3978−3980.
52. Kraulis, P. (1991) *J. Appl. Crystallogr. 24*, 946−950.
53. Merritt, E. A., and Bacon, D. J. (1997) *Methods Enzymol. 277*, 505−524.

BI034986B